Modelling Fractures in Rock

Marco A. Perez
Parex Resources

Summary

The variation in elastic properties in seismic applications has been founded in variations in lithology, porosity, and fluid saturation. However sonic measurements at many scales (well logging, core measurements and seismic data) have shown the dependence of velocity on the propagation direction. Two of the more commonly used models to describe the most demonstrable seismic expressions are the anisotropic symmetries referred to as vertical and horizontal transverse isotropy (VTI and HTI respectively). A mental model for these can be represented as a set of oriented cracks or fractures parallel and perpendicular to bedding. The ability to model the elastic properties as a function of lithology, pore shapes and fractures augments the ability to interpret seismic attributes. In this work, Maxwell's effective field equations (Sevostianov and Kachanov, 2009) are used to model variations in lithology, porosity, and fractures. The model is compared to published ultrasonic data in the manner of Li (2006).

Theory / Method / Workflow

The goal is to model various combination of lithology, porosity and cracks/fractures that may be present within the subsurface. Figure 1 illustrates some rock visuals with potential combinations of spherical porosity, random and oriented cracks.

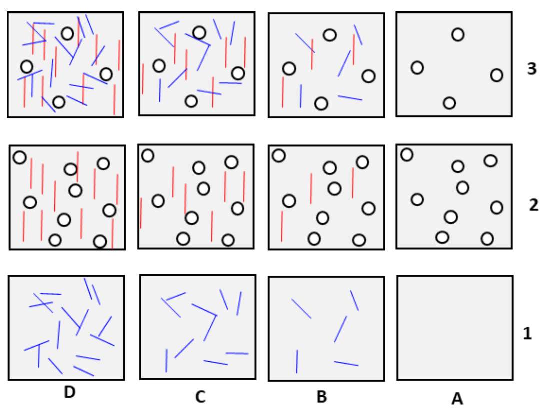

Figure 1. Illustrations of materials with variations in randomly oriented cracks (row 1), concentration of vertical cracks (row 2) and combination of both (row 3). Note that each row contains a different amount of spherical porosity.

To model the elastic property variation observed in rocks, the following expressions are used, following Sevostianov and Kachanov (2009). The elastic properties of E_0, G_0 and v_0 are Young's and shear modulus and Poisson's ratio of the isotropic matrix. The subscripts denote the orientation of each property, with index 3 corresponding to the vertical. The azimuth of vertical fractures is not specified, resulting in expressions for E_1, E_2, G_{13} and G_{23} to be equivalent.

$$E_1 = E_2 = E_0\left[1 + \frac{32(1-\nu_0{}^2)}{3(2-\nu_0)}\frac{\alpha_{11}}{1-p} + \frac{3(1-\nu_0)(9+5\nu_0)}{2(7-5\nu_0)}\frac{p_p}{1-p}\right]^{-1} \quad (1)$$

$$E_3 = E_0\left[1 + \frac{32(1-\nu_0{}^2)}{3(2-\nu_0)}\frac{\alpha_{33}}{1-p} + \frac{3(1-\nu_0)(9+5\nu_0)}{2(7-5\nu_0)}\frac{p_p}{1-p}\right]^{-1} \quad (2)$$

$$G_{12} = G_0\left[1 + \frac{32(1-\nu_0)}{3(2-\nu_0)}\frac{\alpha_{11}}{1-p} + \frac{15(1-\nu_0)}{(7-5\nu_0)}\frac{p_p}{1-p}\right]^{-1} \quad (3)$$

$$G_{13} = G_{23} = G_0\left[1 + \frac{16(1-\nu_0)}{3(2-\nu_0)}\frac{\alpha_{11}+\alpha_{33}}{1-p} + \frac{15(1-\nu_0)}{(7-5\nu_0)}\frac{p_p}{1-p}\right]^{-1} \quad (4)$$

$$\frac{\nu_{12}}{E_1} = \frac{\nu_{31}}{E_3} = \frac{\nu_0}{E_0}\left[1 + \frac{3(1-\nu_0)(1+5\nu_0)}{2\nu_0(7-5\nu_0)}\frac{p_p}{1-p}\right] \quad (5)$$

where

$$\alpha_{11} = 0.5\big(f_1(\tau_v) + f_2(\tau_v)\big)\rho_v + f_1(\tau_h)\rho_h \quad (6)$$

$$\alpha_{33} = \big(f_1(\tau_v)\rho_v + f_2(\tau_h)\rho_h\big) \quad (7)$$

$$f_1(\tau) = \frac{18-\tau(\tau^2+3)e^{-\tau\pi/2}}{6(\tau^2+9)} \quad (8)$$

$$f_2(\tau) = \frac{(\tau^2+3)(3+\tau e^{-\tau\pi/2})}{3(\tau^2+9)} \quad (9)$$

and p_p is spherical porosity while ρ_v and ρ_h are vertical and horizontal crack concentrations and p is the sum of spherical and crack porosity (see Sevostianov and Kachanov, 2009 for more details). The quantity *f* captures the orientation distribution of vertical and horizontal cracks, as a function of τ. Figure 2 illustrates the impact of the variable τ.

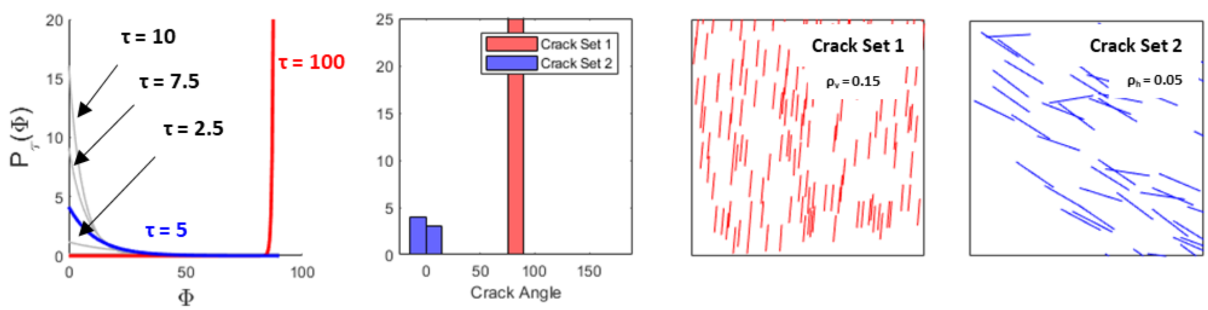

Figure 2. Distribution of two crack sets as a function of τ. As τ increases, the increasingly oriented the fracture distribution becomes.

The crack density tensor α_{ij} is a function of the degree of orientation as well as the concentration of cracks (ρ). In this model the two crack sets are designated to be either vertical or horizontal and thus the notation of α_{11} and α_{33} respectively.

Results, Observations, Conclusions

Figure 3 illustrates the variations in stiffness parameters as a function of porosity, vertical and horizontal crack density, and the degree to which the cracks/fractures are oriented. Results are expressed in terms of vertical P and S wave velocity and Thomsen's VTI parameters.

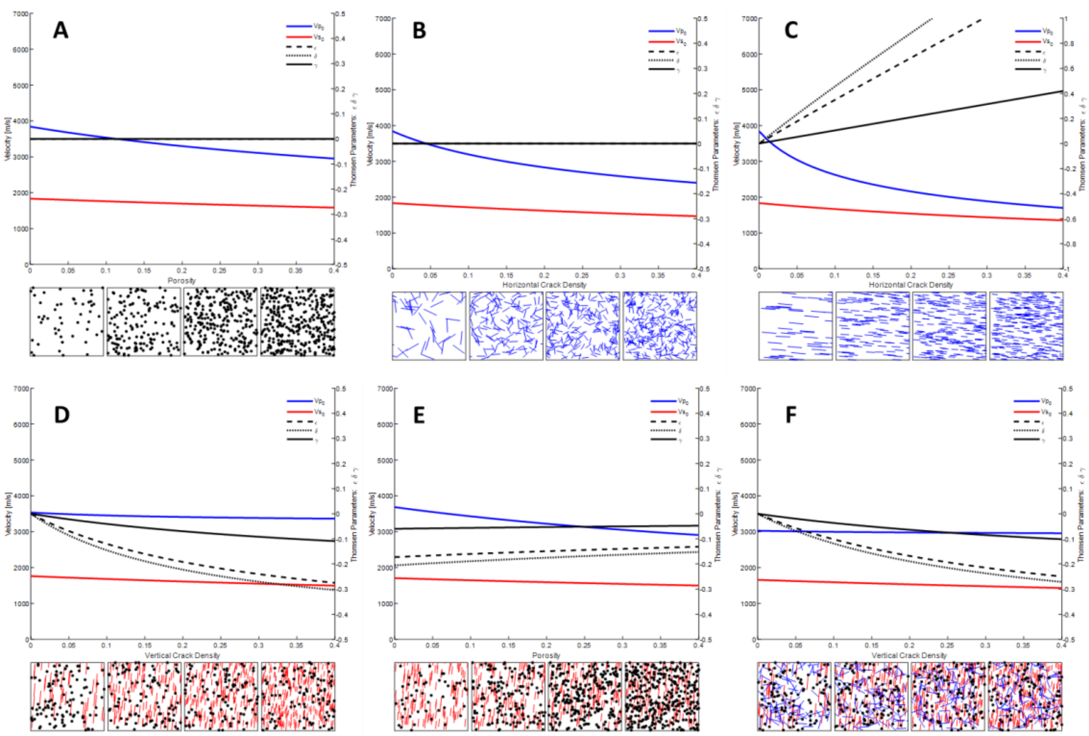

Figure 3. Elastic property variation as a function of A) porosity, B) randomly oriented cracks/fractures C) oriented horizontal fractures, D) vertically oriented fractures with a constant amount of porosity, E) porosity with a constant amount of vertically oriented fractures and F) vertically oriented fractures with a constant amount of porosity and randomly oriented fractures. Below each plot is a representation of pore and/or crack density variation along the x axis.

For the models shown in figure 2, some observations are made. Models A and B are both isotropic with the distinction being the sensitivity of compressional velocity to crack density relative to spherical pores. Compressional velocity difference between B and C show similar sensitivity to the oriented fractures with the addition of Thomsen parameters increasing linearly with fracture concentration. Model D has negative Thomsen parameters, a result of HTI symmetry being expressed in VTI parameters. Model E illustrates the effect porosity has on elastic anisotropy. As porosity increases, Thomsen parameters approach zero, even though vertical fracture concentration has not changed. Finally, model F shows the inability of the vertical compressional velocity to detect variances in vertical fracture concentration.

To close, published ultrasonic data is used to verify model validity, or thought of in a different way, used to calibrate model parameters. Following the displays of Li (2006), figure 3 shows the relationship between compressional and shear velocity to Thomsen's parameters of ε and γ respectively.

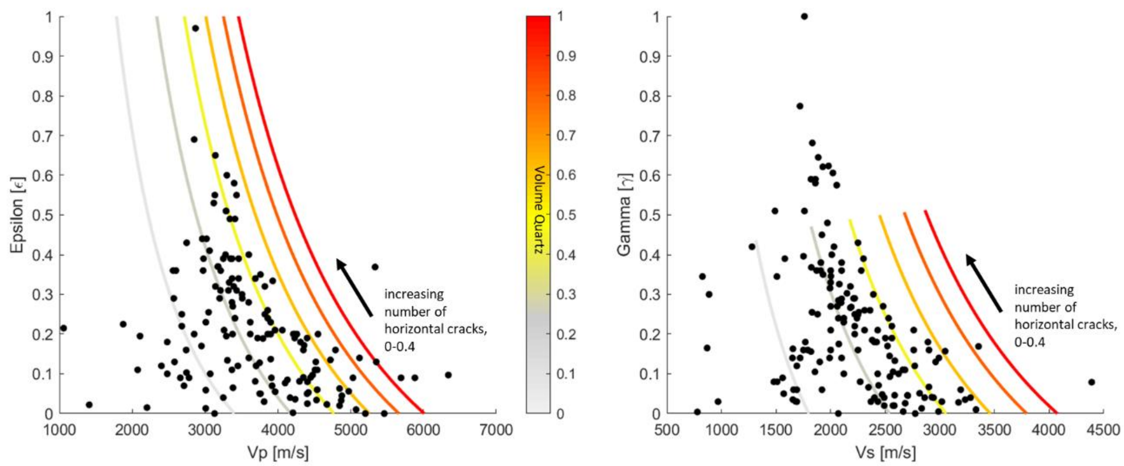

Figure 3. Mixture of Quartz and Clay (moduli as per Li, 2006) at zero porosity. Colors indicate proportion of Quartz volume. Data from Thomsen (1986), Vernik and Nur (1992), Johnston and Christensen (1995) and Vernik and Liu (1997).

The variation in data can be accounted for as a function of porosity, fracture density and lithology. The fracture and lithology variations are displayed in figure 3 showing the potential fits. In this case, the horizontal crack density increase is indicated by the arrow. It is assumed that the matrix components of quartz and clay are isotropic and that any anisotropic effects are only a function of crack density. It is noted that Maxwell's formulation does allow for matrix values to be intrinsically anisotropic, as shown by Sayers, 2013.

Conclusions

Maxwell's formulation has been shown in previous publications to be useful in modelling elastic property variations. The ability to include different pore shapes, geometries and concentrations is suitable for the common models used to interpret seismic data. With core and petrographic data, it is possible to calibrate models to increase prediction accuracy. Moreover, the model can be used to explore a wide variety of what-if scenarios, useful in appropriately understanding interpretation ambiguity.

Acknowledgements

I would like to thank Parex Resources for allowing publication. Thanks to Scott Leaney, Benjamin Roure, Scott Jamieson and Brian Hoffe for helpful discussions.

References

Li, 2006, An emplirical method for estimation of anisotropic parameters in clastic rock, The Leading Edge 706-711
Sayers, 2013, The effect of kerogen on the elastic anisotropy of organic-rich shales, Geophysics 78: D65-D74.
Sevostianov, I., & Kachanov, M. 2009. Elastic and conductive properties of plasma-sprayed ceramic coatings in relation to their microstructure – an overview. Journal of Thermal Spray Technology, 18, 822–834.
Thomsen, L., 1986. Weak elastic anisotropy. Geophysics 51, 1954–1966.
Vernik, L. and A. Nur, 1992, Ultrasonic velocity and anisotropy of hydrocarbon source rocks: Geophysics, **57**, no. 5, 727–735,
Johnston and Christensen (1995) Seismic anisotropy of shales, *JGR*, 1995.
Vernik, L., and X. Liu, 1997, Velocity anisotropy in shales, A petrophysical study: Geophysics, 62, 521–532.